Int. J. Heat Mass Transfer. Vol. 13, pp 1459–1477. Pergamon Press 1970. Printed in Great Britain

A NUMERICAL SOLUTION OF THE MULTIDIMENSIONAL SOLIDIFICATION (OR MELTING) PROBLEM*

ANASTAS LAZARIDIS†
Columbia University, New York, New York, U.S.A.

(*Received* 13 *October* 1969 *and in revised form* 6 *January* 1970)

Abstract—The purpose of this investigation was to develop a simple numerical technique with which to treat heat-transfer problems involving a change of phase. These problems are nonlinear due to the conditions at the moving interface boundary surface. The numerical scheme presented here solves the pertinent equations for the multidimensional problem and determines the temperature distribution in both media around the liquid–solid interface while at the same time it locates the loci of the latter as time progresses.

The types of boundary conditions most frequently encountered in practice are studied in the analysis; the sample problems are selected in such a way as to reflect constant temperature and Newtonian cooling conditions at the boundary of the solidifying substance. The two-dimensional slab and the two- and three-dimensional corners are used to exemplify typical multidimensional geometries.

Comparisons of the results obtained in this work with the few existing solutions show satisfactory agreement.

NOMENCLATURE

$A_1, A_{11}, A_{12}, A_{21}, A_{22}$, coefficients in temperature profile;
a, b, d, terms defining A_{11} and defined by equations (16f, g, h) and (18d, e, f);
Bi_m, Bi_n, Biot numbers at positions $(m\Delta\xi_1, 0)$ and $(0, n\Delta\xi_2)$, respectively;
c_1, c_2, specific heat capacities of solid and liquid phases, respectively;
D, region of space occupied by solidifying matter;
D_1, D_2, parts of space D occupied by solid and liquid phases, respectively;
f, g, functions appearing in the general description of the initial conditions;
h, h_m, h_n, heat-transfer coefficient; subscripts have the same meaning as in Biot numbers;
k_1, k_2, thermal conductivities of solid and liquid phases, respectively;
L, latent heat of fusion;
l_1, l_2, dimensions of cross-section in Example 1;
M, N, number of sections in x and y directions, respectively;
Q_m, Q_n, heat flux at boundary [dimensionless];
R, a convenient reference length;
R_m, interface boundary surface in Fig. 1;
R_{s1}, R_{s2}, fixed boundaries of solid and liquid regions;
S_1, S_2, functions representing boundary conditions over the surfaces R_{s1} and R_{s2};

* This paper is abstracted from the doctoral dissertation of the author, Columbia University, 1969.

† Present address: Research Engineer, E.I. duPont de Nemours & Co., Textile Fibers Department, Pioneering Research Division, Experimental Station, Wilmington, Delaware 19898, U.S.A.

s_1, s_2, expressions of finite difference form used to approximate $\partial T_2/\delta\xi_1$ and $\partial T_1/\partial\xi_1$;
T, T_1, T_2, temperatures;
T_a, T_{a1}, T_{a2}, ambient or surface temperatures; $T_{a1}|_m^0$ is the prescribed surface temperature at the point $(m\Delta\xi_1, 0)$ and time zero;
T_0, initial temperature;
t, t_0, time;
V, solidification temperature;
x, y, space coordinates.

Greek letters

α_1, α_2, thermal diffusivities $(k_1/\rho c_1, k_2/\rho c_2)$;
β, ratio of Biot numbers, Bi_m/Bi_n;
γ_i, ratio of diffusivities (1 when $i = 1$ and α_2/α_1 when $i = 2$);
δ, defines position of interface in the direction of the space variable following it;
Δ, represents increment of variable after it;
$\epsilon_1, \epsilon_2, \epsilon_3$ $(\epsilon_1^*, \epsilon_2^*, \epsilon_3^*)$, position of interface in coordinate directions defined by subscript; the respective dimensionless variables are represented by an asterisk;
θ, dimensionless temperature defined by equation (24);
θ_f, dimensionless fusion temperature;
κ, ratio of conductivities;
λ^*, latent heat parameter, $L/c_1(V - T_a) = \lambda/(V - T_a)$;
$\xi_i(\xi_1, \xi_2, \xi_3)$, coordinate variables [dimensionless];
ρ, density;
σ_i, ratio of $\delta\xi_i/\Delta\xi_i$ [dimensionless];
τ, dimensionless time variable, $\alpha_1 t/R^2$.

INTRODUCTION

The phenomena of melting and freezing are associated with many practical applications of current engineering interest. For example, they are evidenced during the production or melting of ice, the solidification of castings, the freezing of food-stuffs, the aerodynamic heating of missiles and others. The common feature exhibited by all of these problems is the existence of an interface boundary surface which moves either into the solid (melting) or into the liquid region (solidification) in accordance with the relative magnitudes of the temperature gradients on either side of it. The rate at which heat is removed from the solid–liquid interface determines the rate of propagation of that surface; the latter is desired along with the temperature distribution in the solid and the liquid regions at any time during the change of state.

Generally, the problem involves a three-dimensional transient analysis and it is one of considerable mathematical complexity. Heat is absorbed or liberated at the transition region and the thermal properties of the two phases around it are usually different and generally temperature-dependent. A heat balance across the interface indicates that the mathematical model is nonlinear [1, 2]; coupled with it is the fact that the rate of travel of the phase change through the medium is unknown *a priori*. Finally, the various kinds of practical boundary and initial conditions are additional factors which further complicate the mathematics.

The importance of the fusion problem has attracted a large number of investigators who have tried a variety of different techniques to obtain a solution. The literature covers both experimental and theoretical work in this area, but it deals with the one-dimensional geometry almost exclusively [1–3]. Some of this work has involved the study of the one-dimensional problem with cylindrical symmetry [1, 4–8] as well as spherical symmetry [5, 9, 10]. The multidimensional problem seems to have been less popular, probably due to its higher com-

plexity. Only a very limited amount of research has been reported involving the two-dimensional case with some simple geometries and boundary and initial conditions of limited applicability [11–14].

The intent of this work was to obtain a numerical solution of the solidification (melting) problem for a pure substance (or eutectic alloy) in multidimensional space. The problem was considered from the solidification point of view, especially as applied to the freezing of castings. It should be borne in mind, however, that the equations which govern the physical phenomenon are the same for all the problems involving melting or freezing (minor modifications may be necessary). Hence, the method developed in this manuscript is applicable to the entire class of these problems with possible minor modifications in the mathematical equations and the numerical approach.

FORMULATION OF THE PROBLEM

The fusion process for a pure substance (or a eutectic alloy) is described as follows. At time t_0 the two regions D_1 (solid) and D_2 (liquid), which are bounded by the fixed boundary surfaces R_{s1} and R_{s2}, respectively, comprise the domain D of space and are separated through the interface boundary surface R_m (Fig. 1). At the time instant $t = t_0 + \Delta t$ the boundary R_m is another surface in the region D (say, that shown by the dotted lines in the figure) determined by the conditions of the problem (solidification vs. melting). The problem is to locate

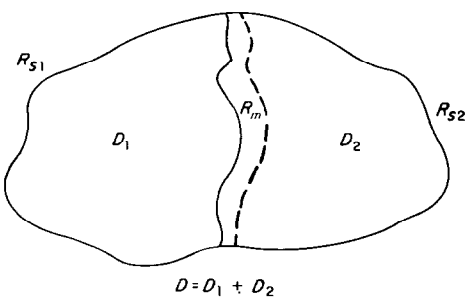

FIG. 1. Graphical presentation of the solidification (or melting) problem.

R_m in space at any time t and subsequently determine the temperature distributions T_1 and T_2 in the two domains D_1 and D_2 respectively.

The mathematical analysis is considerably simplified by the following assumptions:

1. The properties of the materials undergoing melting or freezing can be satisfactorily described by not more than two sets of properties, one for the liquid state and one for the solid state; the density of both phases is assumed to be the same in the neighborhood of the interface.
2. The liquid melt remains stationary so that heat is transferred through it only by conduction.

Thus, the problem is equivalent to solving the heat conduction equation (1) for the temperatures T_1 and T_2 subject to the conditions (2)–(5) at the fixed and moving boundaries and to the initial conditions (6) and (7).

$$\gamma_i \sum_{j=1}^{3} \left(\frac{\partial^2 T_i}{\partial \xi_j^2} \right) = \frac{\partial T_i}{\partial \tau} \qquad i = 1, 2 \tag{1}$$

$$S_1(T_1) = 0 \qquad \text{on} \quad R_{s1} \tag{2}$$

$$S_2(T_2) = 0 \qquad \text{on} \quad R_{s2} \tag{3}$$

at any point $(\epsilon_1, \epsilon_2, \epsilon_3)$ on the interface R_m

$$T_1 = T_2 = V = \text{constant} \tag{4}$$

$$\left[1 + \left(\frac{\partial \epsilon_i^*}{\partial \xi_j} \right)^2 + \left(\frac{\partial \epsilon_i^*}{\partial \xi_k} \right)^2 \right] \left(\frac{\partial T_1}{\partial \xi_i} - \kappa \frac{\partial T_2}{\partial \xi_i} \right) = \lambda \frac{\partial \epsilon_i^*}{\partial \tau}$$

$$i = 1 \quad j = 2 \quad k = 3$$

$$i = 2 \quad j = 3 \quad k = 1$$

$$i = 3 \quad j = 1 \quad k = 2 \tag{5}$$

and at $\tau = 0$

$$T_i = f_i(\xi_j); \quad i = 1, 2, \quad j = 1, 2, 3 \tag{6}$$

$$R_m = g(\xi_j); \quad j = 1, 2, 3 \tag{7}$$

where by using a reference length R all the variables, except λ, T_1 and T_2, are normalized:

$$\lambda = \frac{L}{c_1} \quad \tau = \frac{\alpha_1 t}{R^2} \quad \kappa = \frac{k_2}{k_1} \quad \xi_j = \frac{x_j}{R}$$

$$\epsilon_j^*(\tau) = \frac{\epsilon_j(t)}{R}; \quad j = 1, 2, 3. \tag{8}$$

$$\gamma_i = \begin{cases} 1 & \text{when } i = 1 \\ \dfrac{\alpha_2}{\alpha_1} & \text{when } i = 2. \end{cases}$$

In the above, equations (2), (3), (6) and (7) are general functional representations of the boundary and initial conditions, and equation (5) results as a consequence of a series of mathematical manipulations of the more elaborate energy balance equation at the solid–liquid interface [15, 16]. The nonlinear behavior of the mathematical model is due to the presence of the energy balance relation; the usefulness of the reduced equation (5) is realized when the observation is made that the motion of the fusion front can be treated as quasi-one-dimensional, the temperature gradients being taken in one direction only.

MATHEMATICAL ANALYSIS

An auxiliary set of differential equations is derived in this section by reference to the condition that the interface is an isothermal surface. First, the time rate of change of the temperatures T_1 and T_2 vanishes at the interface; thus, equation (9) is obtained.

$$\gamma_i \sum_{j=1}^{3} \frac{\partial^2 T_i}{\partial \xi_j^2} + \frac{\partial T_i}{\partial \xi_k} \frac{\partial \epsilon_k^*}{\partial \tau} = 0; \quad k = 1, 2, 3. \tag{9}$$

Then, two consecutive differentiations of T_1 and T_2 along lines tangent to the interface yield equations (10)–(12):

$$\frac{\partial T_k}{\partial \xi_i} + \frac{\partial T_k}{\partial \xi_j} \frac{\partial \epsilon_j^*}{\partial \xi_i} = 0 \tag{10}$$

$$\frac{\partial^2 T_k}{\partial \xi_i^2} + 2 \frac{\partial^2 T_k}{\partial \xi_i \partial \xi_j} \frac{\partial \epsilon_j^*}{\partial \xi_i} + \frac{\partial T_k}{\partial \xi_j} \frac{\partial^2 \epsilon_j^*}{\partial \xi_i^2} + \frac{\partial^2 T_k}{\partial \xi_j^2} \left(\frac{\partial \epsilon_j^*}{\partial \xi_i} \right)^2 = 0 \tag{11}$$

where $j = 1$ and $i = 2, 3$
$j = 2$ and $i = 1, 3$
$j = 3$ and $i = 1, 2$

and

$$\frac{\partial^2 T_k}{\partial \xi_i \partial \xi_j} + \frac{\partial^2 T_k}{\partial \xi_i \partial \xi_m} \left(\frac{\partial \epsilon_m^*}{\partial \xi_j} \right) + \frac{\partial^2 T_k}{\partial \xi_j \partial \xi_m} \left(\frac{\partial \epsilon_m^*}{\partial \xi_i} \right) + \frac{\partial^2 T_k}{\partial \xi_m^2} \left(\frac{\partial \epsilon_m^*}{\partial \xi_i} \right) \left(\frac{\partial \epsilon_m^*}{\partial \xi_j} \right) + \frac{\partial T_k}{\partial \xi_m} \left(\frac{\partial^2 \epsilon_m^*}{\partial \xi_i \partial \xi_j} \right) = 0 \tag{12}$$

where $i = 1$ and $j = 2$ and $m = 3$
$i = 2$ and $j = 3$ and $m = 1$
$i = 3$ and $j = 1$ and $m = 2$

and $k = 1, 2.$

The convenience of handling these expressions will be apparent later with the development of a numerical scheme which will deal with the interface motion along lines parallel to the coordinate axes and not along lines normal to itself.

NUMERICAL ANALYSIS

The finite difference approximations of both the implicit and the explicit types have been used in various numerical techniques developed previously. Most of these, however, have been applied to one-dimensional solidification problems and they have not been extended to cover multidimensional conditions.† In this manuscript the explicit finite difference technique is adopted [17, 18] for all nodes sufficiently far from the interface and a special scheme is devised for points close to it.‡

To begin the numerical study, a network of lines is passed through the medium under consideration. For the sake of simplicity, a two-dimensional configuration will be considered in the following (cf. Fig. 2). Now, suppose that at time τ, the interface is known to be the curve

† A concise summary of previous methods can be found in [3].

‡ Only the highlights of the method are presented here; the details can be found in [15].

AB in Fig. 2. Any point on this curve can be identified and traced in relation to a nodal point which neighbors it. The latter have been chosen to lie on the left and/or below the curve. Let one such node be the point $P(p\Delta\xi_1, q\Delta\xi_2)$. Its distance from and to the left of the fusion front is denoted by $\delta\xi_1$ and that below by $\delta\xi_2$.

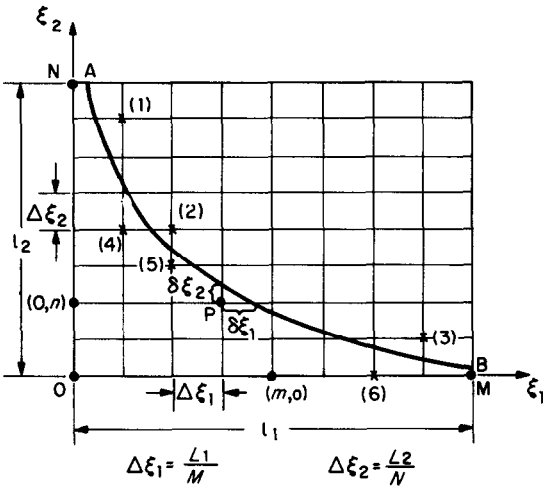

FIG. 2. Finite difference grid of a plane surface showing interface curve AB and defining some terms used in the paper.

The temperatures of all nodes $(m\Delta\xi_1, n\Delta\xi_2)$ located far enough from the interface are computed by the finite difference expression (13) of the explicit type.

$$T_{mn}^{k+1} = T_{mn}^{k}\left[1 - \frac{2\gamma_i\Delta\tau}{(\Delta\xi_1)^2}\left(1 + \frac{\Delta\xi_1^2}{\Delta\xi_2^2}\right)\right] + \frac{\gamma_i\Delta\tau}{\Delta\xi_1^2}\left[T_{m+1,n}^{k} + T_{m-1,n}^{k} + \left(\frac{\Delta\xi_1}{\Delta\xi_2}\right)^2 (T_{m,n+1}^{k} + T_{m,n-1}^{k})\right] \quad (13)$$

where γ_i has the meaning ascribed to it earlier and

$$m = 1, 2, \ldots, p-1, p+2, \ldots, M-1$$
$$n = 1, 2, \ldots, q-1, q+2, \ldots, N-1.$$

Care must be exercised with the selection of the time increment in equation (13) so that the coefficient of T_{mn}^{k} is positive; otherwise, the scheme may turn out to be unstable.

Near the interface the derivatives of equations (9)–(12) are approximated by second order finite difference expressions; for example, if $\sigma_i = \delta\xi_i/\Delta\xi_i$, $i = 1, 2$,

$$\left.\frac{\partial T_2}{\partial\xi_i}\right|_{\epsilon_1,\epsilon_2} = \left[\frac{2-\sigma_i}{1-\sigma_i}T_{p+1,q} - \frac{(3-2\sigma_i)V}{(1-\sigma_i)(2-\sigma_i)} - \frac{1-\sigma_i}{2-\sigma_i}T_{p+2,q}\right]\left(\frac{1}{\Delta\xi_i}\right). \quad (14)$$

These relations are singular at $\sigma_i = 0$ for T_1 and at $\sigma_i = 1$ for T_2. However, the singularities can be avoided by means of the following technique. When a node is neighboring with the interface, its temperature is represented by a quadratic profile of the form

$$T = A_{11}(\xi_1 - \epsilon_1^*) + A_{12}(\xi_1 - \epsilon_1^*)^2 + A_{21}(\xi_2 - \epsilon_2^*) + A_{22}(\xi_2 - \epsilon_2^*)^2 + A_1(\xi_1 - \epsilon_1^*)(\xi_2 - \epsilon_2^*) + V. \quad (15)$$

This approach has a truncation error of the same order of magnitude as the finite difference expressions of the type (14). Four cases are distinguished based on whether $\sigma_i \leqslant \frac{1}{2}$ or $\sigma_i > \frac{1}{2}$.† For instance, if $0 \leqslant \sigma_1 \leqslant \frac{1}{2}$, then

$$T_{p,q}^{k+1} = [A_{12}(\delta\xi_1) - A_{11}](\delta\xi_1) + V \quad (16)$$

and

$$A_{11} = -\frac{b}{2a} + \sqrt{\left[\left(\frac{b}{2a}\right)^2 - \frac{d}{a}\right]} \quad (16a)$$

$$A_{12} = \left(\frac{T_{p-1,q}^{k+1} - V}{\delta\xi_1 + \Delta\xi_1} + A_{11}\right)\Big/(\delta\xi_1 + \Delta\xi_1) \quad (16b)$$

$$A_{21} = -A_{11}(\partial\epsilon_1^*/\partial\xi_2) \quad (16c)$$

$$A_{22} = -A_{12} - \frac{1}{2\lambda}\left[1 + \left(\frac{\partial\epsilon_1^*}{\partial\xi_2}\right)^2\right] \times A_{11}(A_{11} - \kappa s_1) \quad (16d)$$

† Six cases in the event a three-dimensional problem is considered.

$$A_1 = \left\{\frac{A_{11}}{\lambda}(A_{11} - \kappa s_1)\left[1 + \left(\frac{\partial \epsilon_1^*}{\partial \xi_2}\right)^2\right] - A_{11}\frac{\partial^2 \epsilon_1^*}{\partial \xi_2^2} + 2A_{12}\left[1 - \left(\frac{\partial \epsilon_1^*}{\partial \xi_2}\right)^2\right]\right\} \div \left[2\left(\frac{\partial \epsilon_1^*}{\partial \xi_2}\right)\right] \tag{16e}$$

where

$$a = \Delta\xi_2\left[\delta\xi_1 - \left(\frac{\partial \epsilon_1^*}{\partial \xi_2}\right)\Delta\xi_2\right]\left[1 + \left(\frac{\partial \epsilon_1^*}{\partial \xi_2}\right)^2\right] \tag{16f}$$

$$b = \frac{2\lambda}{\delta\xi_1 + \Delta\xi_1}\left\{(\delta\xi_1)(\Delta\xi_2) + (\Delta\xi_1)(\Delta\xi_2)\left(\frac{\partial \epsilon_1^*}{\partial \xi_2}\right)^2 - \left(\frac{\partial \epsilon_1^*}{\partial \xi_2}\right)[(\Delta\xi_2)^2 + (\Delta\xi_1)(\delta\xi_1)]\right\} - \lambda\left(\frac{\partial^2 \epsilon_1^*}{\partial \xi_2^2}\right)(\delta\xi_1)(\Delta\xi_2) - \kappa a s_1 \tag{16g}$$

$$d = 2\lambda\left\{\frac{T_{p-1,q}^{k+1} - V}{(\delta\xi_1 + \Delta\xi_1)^2}\left[\left(\frac{\partial \epsilon_1^*}{\partial \xi_2}\right)\{(\delta\xi_1)^2 - (\Delta\xi_2)^2\}\right] + \left(\frac{\partial \epsilon_1^*}{\partial \xi_2}\right)(V - T_{p,q-1}^{k+1}) + \left[1 - \left(\frac{\partial \epsilon_1^*}{\partial \xi_2}\right)^2\right](\delta\xi_1)(\Delta\xi_2)\frac{(T_{p-1,q}^{k+1} - V)}{(\delta\xi_1 + \Delta\xi_1)^2}\right\} \tag{16h}$$

and s_1 represents the finite difference approximation of the form of equation (14) for $(\partial T_2/\partial \xi_1)$ at $(\epsilon_1^*, \epsilon_2^*)$. Finally,

$$T_{p+1,q}^{k+1} = \left\{1 - \frac{2\gamma_2\Delta\tau}{\Delta\xi_1^2}\left[\frac{1}{1-\sigma_1} + \frac{(\Delta\xi_1/\Delta\xi_2)^2}{1-\sigma_2}\right]\right\}T_{p+1,q}^k + \frac{2\gamma_2\Delta\tau}{\Delta\xi_1^2}\left\{V\left[\frac{1}{(2-\sigma_1)(1-\sigma_1)} + \frac{(\Delta\xi_1/\Delta\xi_2)^2}{(2-\sigma_2)(1-\sigma_2)}\right] + \frac{T_{p+2,q}^k}{2-\sigma_1} + \left(\frac{\Delta\xi_1}{\Delta\xi_2}\right)^2\left(\frac{T_{p+1,q+1}^k}{2-\sigma_2}\right)\right\} \tag{17a}$$

when the node $Q[(p+1)\Delta\xi_1, q\Delta\xi_2]$ is a point like (2) in Fig. 2, or

$$T_{p+1,q}^{k+1} = \left\{1 - \frac{2\gamma_2\Delta\tau}{\Delta\xi_1^2}\left[\frac{1}{1-\sigma_1} + \left(\frac{\Delta\xi_1}{\Delta\xi_2}\right)^2\right]\right\}T_{p+1,q}^k + \frac{2\gamma_2\Delta\tau}{\Delta\xi_1^2}\left[\frac{1}{2-\sigma_1}\left(T_{p+2,q}^k + \frac{V}{1-\sigma_1}\right) + \frac{1}{2}\left(\frac{\Delta\xi_1}{\Delta\xi_2}\right)^2(T_{p+1,q+1}^k + T_{p+1,q-1}^k)\right] \tag{17b}$$

when $Q[p+1)\Delta\xi_1, q\Delta\xi_2]$ is a point like (1). On the other hand, if $\frac{1}{2} < \sigma_1 \leqslant 1$, then

$$T_{p+1,q}^{k+1} = [A_{11} + A_{12}(1-\sigma_1)\Delta\xi_1] \times (1-\sigma_1)\Delta\xi_1 + V \tag{18}$$

and, A_{11} and A_{21} are given by equations (16a) and (16c), respectively,

$$A_{12} = \left[\frac{T_{p+2,q}^{k+1} - V}{2\Delta\xi_1 - \delta\xi_1} - A_{11}\right]\Big/(2\Delta\xi_1 - \delta\xi_1) \tag{18a}$$

$$A_{22} = -A_{12} - \frac{1}{2\lambda\gamma_2}\left[1 + \left(\frac{\partial \epsilon_1^*}{\partial \xi_2}\right)^2\right] \times A_{11}(s_2 - \kappa A_{11}) \tag{18b}$$

$$A_1 = \left[\left[2A_{12}\left[1 - \left(\frac{\partial \epsilon_1^*}{\partial \xi_2}\right)^2\right] + A_{11} \times \left[\frac{s_2}{\lambda\gamma_2}\left\{1 + \left(\frac{\partial \epsilon_1^*}{\partial \xi_2}\right)^2\right\} - \frac{\partial^2 \epsilon_1^*}{\partial \xi_2^2}\right] - \frac{\kappa}{\lambda\gamma_2}\left[1 + \left(\frac{\partial \epsilon_1^*}{\partial \xi_2}\right)^2\right]A_{11}\right]\Big/\left[2\left(\frac{\partial \epsilon_1^*}{\partial \xi_2}\right)\right] \tag{18c}$$

where

$$a = \frac{\kappa(\Delta\xi_2)}{\gamma_2}\left[1 + \left(\frac{\partial\epsilon_1^*}{\partial\xi_2}\right)^2\right]\left[\Delta\xi_2\left(\frac{\partial\epsilon_1^*}{\partial\xi_2}\right) - (\Delta\xi_1 - \delta\xi_1)\right] \quad (18d)$$

$$b = 2\lambda\left\{\left(\frac{\partial\epsilon_1^*}{\partial\xi_2}\right)\left[\frac{1 - \sigma_1 + (\Delta\xi_2/\Delta\xi_1)^2}{2 - \sigma_1}\right](\Delta\xi_2) - \left(\frac{\partial\epsilon_1^*}{\partial\xi_2}\right)^2\left(\frac{\Delta\xi_2}{2 - \sigma_1}\right) - \Delta\xi_2\left(\frac{1 - \sigma_1}{2 - \sigma_1}\right)\right\} - \lambda\left(\frac{\partial^2\epsilon_1^*}{\partial\xi_2^2}\right)(\Delta\xi_2)(\Delta\xi_1 - \delta\xi_1) - \frac{s_2 a}{\kappa} \quad (18e)$$

$$d = 2\lambda\left\{\left(\frac{\partial\epsilon_1^*}{\partial\xi_2}\right)(V - T^{k+1}_{p+1,q+1}) + \frac{T^{k+1}_{p+2,q} - V}{(2\Delta\xi_1 - \delta\xi_1)^2}\left[\left(\frac{\partial\epsilon_1^*}{\partial\xi_2}\right)\{(\Delta\xi_1 - \delta\xi_1)^2 - (\Delta\xi_2)^2\} + \left\{1 - \left(\frac{\partial\epsilon_1^*}{\partial\xi_2}\right)^2\right\} \times (\Delta\xi_2)(\Delta\xi_1 - \delta\xi_1)\right]\right\} \quad (18f)$$

and s_2 represents the finite difference approximation for $(\partial T_1/\partial\xi_1)$ at $(\epsilon_1^*, \epsilon_2^*)$. Finally,

$$T^{k+1}_{p,q} = \left\{1 - \frac{2\Delta\tau}{\Delta\xi_1^2}\left[\frac{1}{\sigma_1} + \frac{(\Delta\xi_1/\Delta\xi_2)^2}{\sigma_2}\right]\right\}T^k_{p,q} + \frac{2\Delta\tau}{\Delta\xi_1^2}\left\{V\left[\frac{1}{\sigma_1(1 + \sigma_1)} + \frac{(\Delta\xi_1/\Delta\xi_2)^2}{\sigma_2(1 + \sigma_2)}\right] + \frac{T^k_{p-1,q}}{1 + \sigma_1} + \left(\frac{\Delta\xi_1}{\Delta\xi_2}\right)^2\frac{T^k_{p,q-1}}{1 + \sigma_2}\right\} \quad (19a)$$

when the node $P(p\Delta\xi_1, q\Delta\xi_2)$ is a point like (5) in Fig. 2, or

$$T^{k+1}_{p,q} = \left\{1 - \frac{2\Delta\tau}{\Delta\xi_1^2}\left[\frac{1}{\sigma_1} + \left(\frac{\Delta\xi_1}{\Delta\xi_2}\right)^2\right]\right\}T^k_{p,q} + \frac{2\Delta\tau}{\Delta\xi_1^2}\left[\frac{V}{\sigma_1(1 + \sigma_1)} + \frac{T^k_{p-1,q}}{1 + \sigma_1} + \frac{1}{2}\left(\frac{\Delta\xi_1}{\Delta\xi_2}\right)^2 \times (T^k_{p,q-1} + T^k_{p,q+1})\right] \quad (19b)$$

when $P(p\Delta\xi_1, q\Delta\xi_2)$ is a point like (4), or

$$T^{k+1}_{p,q} = \left\{1 - \frac{2\Delta\tau}{\Delta\xi_1^2}\left[1 + \frac{(\Delta\xi_1/\Delta\xi_2)^2}{\sigma_2}\right]\right\}T^k_{p,q} + \frac{2\Delta\tau}{\Delta\xi_1^2}\left\{\frac{1}{2}(T^k_{p-1,q} + T^k_{p+1,q}) + \left(\frac{\Delta\xi_1}{\Delta\xi_2}\right)^2\left[\frac{V}{\sigma_2} + T^k_{p,q-1}\right](1 + \sigma_2)^{-1}\right\} \quad (19c)$$

when $P(p\Delta\xi_1, q\Delta\xi_2)$ is a point like (6) in Fig. 2. Similar relations are obtained for σ_2 (and σ_3 in the three-dimensional case) in the ranges 0–0·5 and 0·5–1, respectively.

The numerical equations developed for the conditions at the fixed boundaries are presented next. When the interface is away from the boundaries, equation (13) gives the temperatures of the nodes near these boundaries. When a boundary is exposed to convection heat transfer, the boundary temperatures are calculated by means of one of the following three equations:

(a) $m \neq 0, n = 0$

$$T^{k+1}_{mn} = \left\{\left[1 - \frac{2\gamma_i\Delta\tau}{\Delta\xi_1^2}\left(1 + \frac{\Delta\xi_1^2}{\Delta\xi_2^2}\right) - \frac{\gamma_i\Delta\tau}{\Delta\xi_2}Bi_m\right]T^k_{mn} + \frac{\gamma_i\Delta\tau}{\Delta\xi_1^2}\left[T^k_{m-1,n} + T^k_{m+1,n} + 2\left(\frac{\Delta\xi_1}{\Delta\xi_2}\right)^2(T^k_{m,n+1} + Bi_m\Delta\xi_2 T_a)\right] + \frac{2\gamma_i\Delta\tau}{\Delta\xi_2}Q_m\right\}\Big/\left(1 + \frac{Bi_m\gamma_i\Delta\tau}{\Delta\xi_2}\right) \quad (20a)$$

(b) $m = 0, n \neq 0$

$$T^{k+1}_{mn} = \left\{\left[1 - \frac{2\gamma_i\Delta\tau}{\Delta\xi_1^2}\left(1 + \frac{\Delta\xi_1^2}{\Delta\xi_2^2}\right) - \frac{\gamma_i\Delta\tau}{\Delta\xi_1}Bi_n\right]T^k_{mn} + \frac{\gamma_i\Delta\tau}{\Delta\xi_1^2}\left[2(T^k_{m+1,n} + Bi_n\Delta\xi_1 T_a) + \left(\frac{\Delta\xi_1}{\Delta\xi_2}\right)^2(T^k_{m,n-1} + T^k_{m,n+1})\right] + \frac{2\gamma_i\Delta\tau}{\Delta\xi_1}Q_n\right\}\Big/\left(1 + \frac{Bi_n\gamma_i\Delta\tau}{\Delta\xi_1}\right) \quad (20b)$$

(c) $m = 0, n = 0$

$$T_{mn}^{k+1} = \left\{\left[1 - \frac{2\gamma_i\Delta\tau}{\Delta\xi_1^2}\left(1 + \frac{\Delta\xi_1^2}{\Delta\xi_2^2}\right) - \frac{\gamma_i\Delta\tau}{\Delta\xi_1} Bi_n\left(1 + \frac{\Delta\xi_1}{\Delta\xi_2}\beta\right)\right] T_{mn}^k + \frac{2\gamma_i\Delta\tau}{\Delta\xi_1^2}\left[T_{m+1,n}^k + \left(\frac{\Delta\xi_1}{\Delta\xi_2}\right)^2 T_{m,n+1}^k + \Delta\xi_1(Bi_n T_a + Q_n) + \frac{\Delta\xi_1^2}{\Delta\xi_2}(Bi_m T_a + Q_m)\right]\right\} \Big/ \left[1 + \frac{\gamma_i\Delta\tau}{\Delta\xi_1} Bi_n\left(1 + \frac{\Delta\xi_1}{\Delta\xi_2}\beta\right)\right] \quad (20c)$$

where $Bi_m = h_m R/k_1$, $Bi_n = h_n R/k_1$, and $\beta = Bi_m/Bi_n$. The terms involving Q_m and Q_n have been added in order to include the case of a heat flux imposed on the boundaries.

If the interface is between the boundary and the first node from it, a different set of equations of the form (16)–(19c) is used for each type of boundary conditions.† Finally, a word must be said about the procedure used to start the calculations of the solid–liquid interface motion. Thus, when the boundary temperatures are prescribed, the solidification front at the first time step is calculated from the simultaneous solution of the equations

$$\delta\xi_{1n} = \left[1 + \left(\frac{\partial\epsilon_1^*}{\partial\xi_2}\right)^2\right]\frac{\Delta\tau}{\lambda\Delta\xi_1}\left[\frac{V - T_{a2}|_n^0}{\sigma_1} - \kappa\frac{(3 - 2\sigma_1)(T_0 - V)}{(1 - \sigma_1)(2 - \sigma_1)}\right] \quad (21a)$$

$$0 < n \leqslant N$$

and

$$\delta\xi_{2m} = \left[1 + \left(\frac{\partial\epsilon_2^*}{\partial\xi_1}\right)^2\right]\frac{\Delta\tau}{\lambda\Delta\xi_2}\left[\frac{V - T_{a2}|_m^0}{\sigma_2} - \kappa\frac{(3 - 2\sigma_2)(T_0 - V)}{(1 - \sigma_2)(2 - \sigma_2)}\right], \quad 0 < m \leqslant M \quad (21b)$$

† These expressions can be found in [15] together with details for their derivation.

where the proper σ_1 and σ_2 are selected for every m and n and the space derivatives of ϵ_1^* and ϵ_2^* are substituted by suitable finite difference approximations. Similarly, in the case of Newtonian cooling at the boundaries, the initial displacement of the interface is computed from the equations

$$\delta\xi_{1n} = \frac{\Delta\tau}{\lambda}\left[Bi_n(V - T_a) - \frac{\kappa}{2\Delta\xi_1}(4T_{1,n} - 3V - T_{2,n})\right] \quad (22a)$$

and

$$\delta\xi_{2m} = \frac{\Delta\tau}{\lambda}\left[Bi_m(V - T_a) - \frac{\kappa}{2\Delta\xi_2}(4T_{m,1} - 3V - T_{m,2})\right]. \quad (22b)$$

The numerical scheme of the three-dimensional case is similar to that applicable to the two-dimensional situation presented above, except for the additional terms which complicate the mathematics further. Nevertheless, a few minor modifications in the numerical technique are able to accommodate the presence of the additional terms so that the method of approach is essentially the same as before. To avoid repetition, the analysis associated with the three-dimensional problem is not covered here and the interested reader is referred to the author's doctoral dissertation [15].

SAMPLE PROBLEMS AND DISCUSSION OF RESULTS

Before proceeding with the presentation of examples, it is advantageous to transform the variables T_1 and T_2, and the parameter λ to dimensionless quantities. This is accomplished by the definitions

$$\lambda^* = \lambda/(V - T_a) \quad (23)$$

and

$$\theta = (T - T_a)/(T_o - T_a) \quad (24)$$

where T is either T_1 or T_2 and T_a is chosen to be either the prescribed boundary temperature or

the ambient temperature. The symbol θ_f will appear frequently in the graphical presentation of the results and in the discussion below; it represents the dimensionless fusion temperature and its definition follows directly from equation (24), where now the fusion temperature V substitutes for the variable T.

Example 1. A prism of square cross-section is in the liquid state at the fusion temperature and it solidifies due to a constant temperature, lower than the solidification temperature, maintained at the surface of the prism.

First, the numerical results for the infinite corner are combined in the generalized curve of Fig. 3 for the depth of solidification. This graph represents a similarity solution of the same form as Stefan's solution of the one-dimensional problem and it shows that the interface is a function of the parameters $\xi_1/\sqrt{\tau}$ and λ^*.† Discrepancies in the positions of the points in this figure reflect numerical errors at the onset of the computations which diminish as time progresses.

Subsequently, the results for the finite square

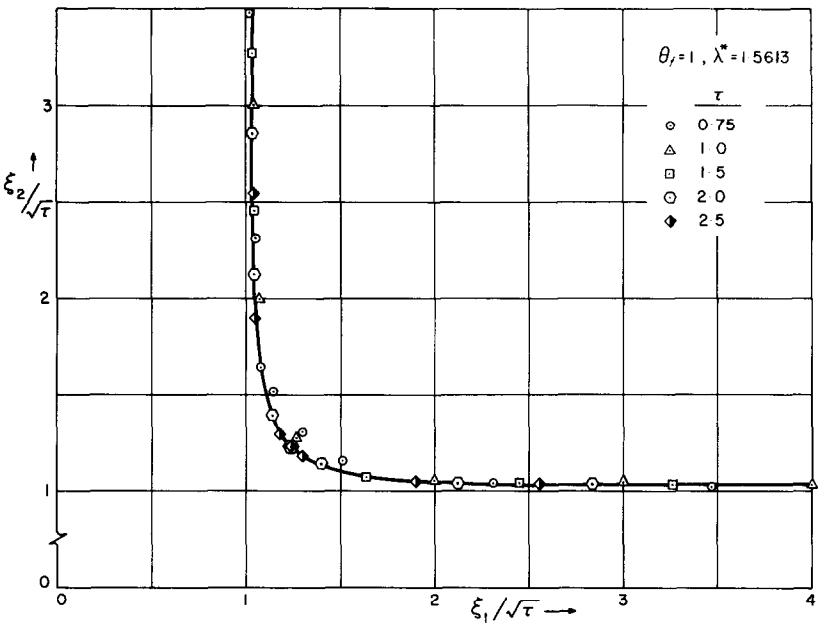

FIG. 3. Similarity solution for the solidifying infinite corner initially at the melting temperature.

The symmetry of this problem allows the simplification of considering only one quarter of the cross-section with two boundaries maintained at the prescribed constant temperature while the others are kept insulated. The numerical data selected for this example were those used in [12] and [13], i.e. $\lambda^* = 1{\cdot}5613$, $\theta_f = 1$, and $l_1 = l_2 = 4$ where l_1 and l_2 are the normalized dimensions of the quarter square section and also the number of nodes if $\Delta\xi_1 = \Delta\xi_2 = 1$.

section are presented in Figs. 4–7. The loci of the interface are shown at several times as solidification progresses in Fig. 4, from which the fraction of the solidified matter along the diagonal and at the insulated boundaries are obtained and plotted vs. the dimensionless time in Figs. 5 and 6, respectively. An examination of

† In general, it is a function of $\xi_1/\sqrt{\tau}$, $\xi_2/\sqrt{\tau}$ and λ^*; however, in this case it is dependent on two parameters only because of symmetry.

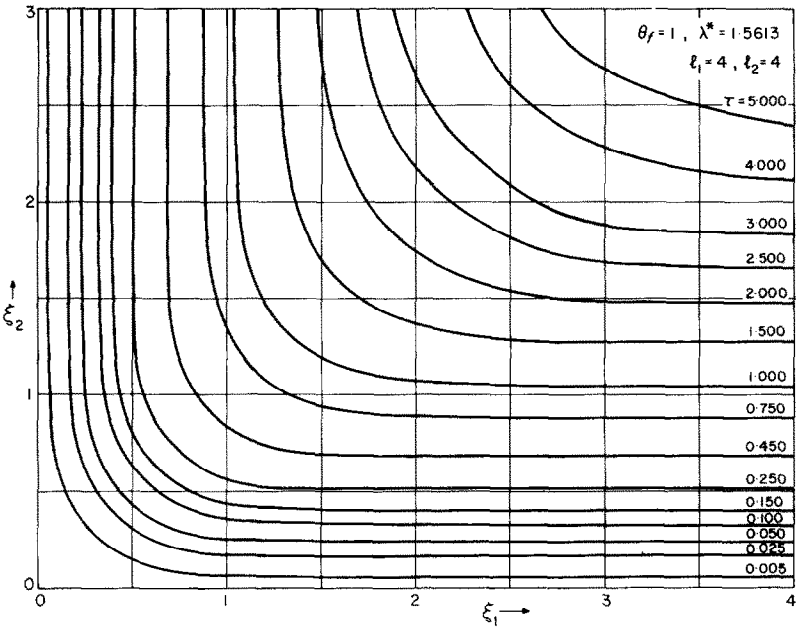

FIG. 4. Loci of interface at several times τ for a square plate initially at the melting temperature.

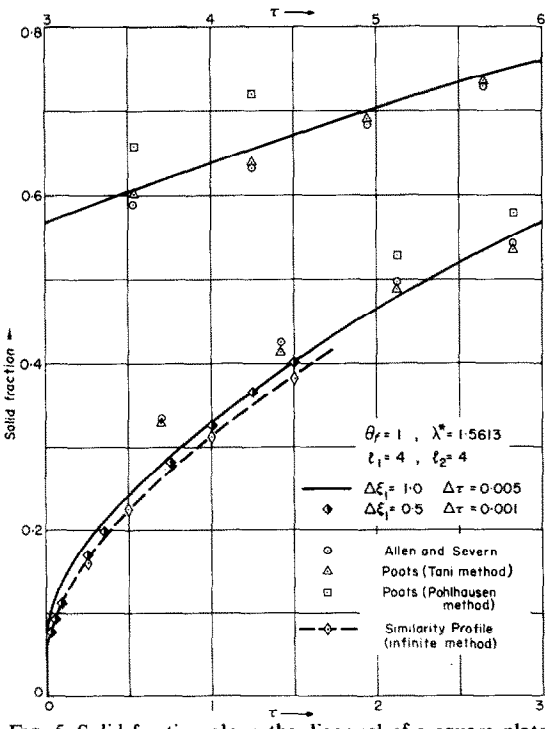

FIG. 5. Solid fraction along the diagonal of a square plate initially at the fusion temperature as a function of time.

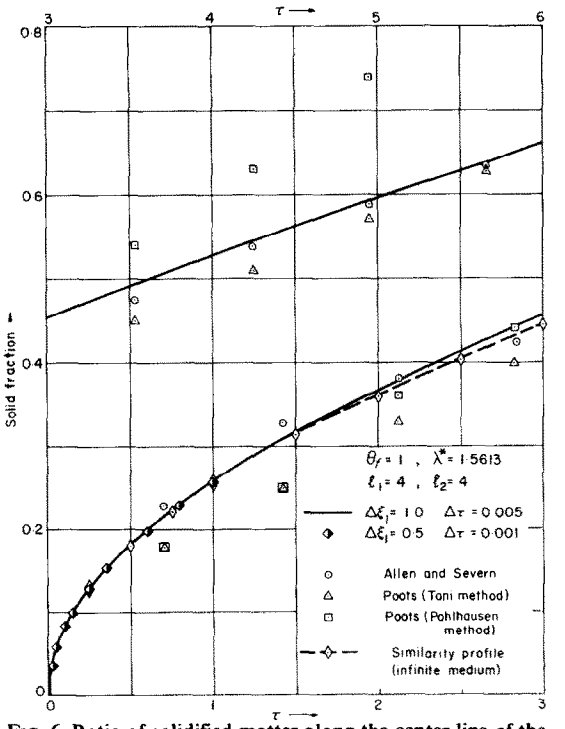

FIG. 6. Ratio of solidified matter along the center line of the square plate of Figs. 4 and 5 vs. time.

these figures reveals that at the later times the results of this investigation compare favorably with those of Allen and Severn [12] and Poots [13] while initially the discrepancies observed are quite large.† Although the present method is approximate, as are both of the previous studies, the following discussion indicates that the results obtained here are the most accurate.

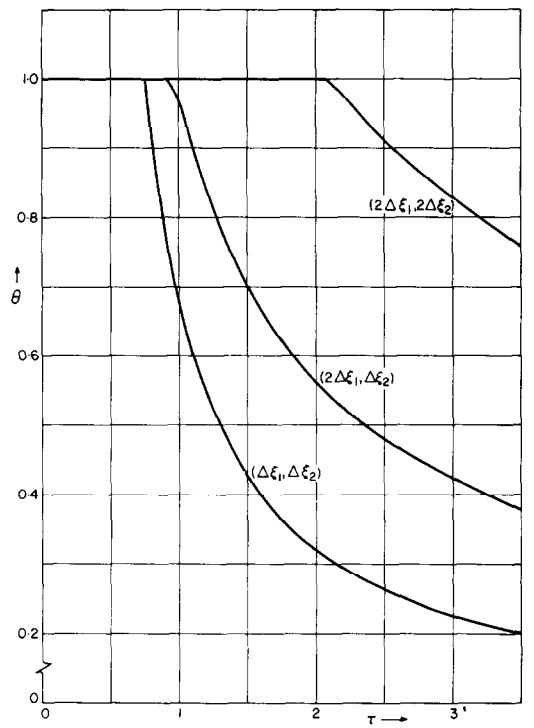

FIG. 7. Temperature histories of some of the nodes in the square plate.

First, Allen and Severn considered the latent heat of fusion as heat generation apportioned to the various modes as a fraction of the area, $h^2 = (\Delta x)(\Delta y)$, depending on the location of the interface. The numerical value of their time increment was such that only 13 time steps were sufficient to solidify the slab. In the present procedure the time increment was chosen to be $\Delta\tau = 0{\cdot}005$ so that the number of time steps required for the complete solidification of the slab exceeded 1000. In addition, the results of Allen and Severn manifest an abnormal behavior of the interface motion and this, perhaps, may be attributed to computational inaccuracies. It is reasonable to expect that the interface curves converge closer and closer to each other as time progresses since the resistance to heat flow out of the slab increases with time. Nonetheless, this is not the case in Fig. 2 of [12].† On the other hand, Poots assumed that the interface for such a configuration is a circle and he obtained two solutions by the approximate techniques of Pohlhausen and Tani, respectively [13]. It was then pointed out that the more accurate results of the Tani technique manifested a maximum error of about 13 per cent at the end of freezing compared with those of Allen and Severn.

During the initial steps of solidification, the similarity solution for the infinite corner is also the solution for the finite slab. This has been plotted in Figs. 5 and 6 for comparison. The latter figure indicates that end effects start to be pronounced in the infinite slab at $\tau = 1{\cdot}0$. Hence, the solution for the finite slab in Fig. 5 must also approach the similarity curve in the time range $0 \leqslant \tau < 1{\cdot}0$ and any discrepancies must be attributed to starting errors in the former. It is evident from this figure that although these discrepancies are present, the solution obtained with $\Delta\xi_1 = \Delta\xi_2 = 1$ and $\Delta\tau = 0{\cdot}005$ is closer to the similarity curve than any of the other two references. What is more important is that the results obtained with $\Delta\xi_1 = \Delta\xi_2 = 0{\cdot}5$ and $\Delta\tau = 0{\cdot}001$ start along the similarity curve and move out as time progresses to join the curve obtained with $\Delta\xi_1 = \Delta\xi_2 = 1$ and $\Delta\tau = 0{\cdot}005$. It can, thus, be concluded that the present method is convergent and gives the most accurate results of all three. Finally, in Fig. 7 the temperature histories of a few selected nodes in the slab are also shown for completeness.

† The maximum relative error based on the results of this investigation is 18 and 16 per cent with [12] and [13], respectively.

† Reference is also made to Table IV-4 of the author's dissertation [15].

Example 2. A liquid metal is poured into a cast of square cross-section. It is required to study the freezing process in the cast if it is initially at a uniform temperature above the melting point and its surface is maintained symmetrically at the constant temperatures T_{a1} and/or T_{a2}, where at least one of them is lower than the fusion temperature. It is assumed that the cast is large enough so that end effects are not important (infinite corner).

boundary temperature is prescribed. Thus, the only parameters of the problem are κ, γ_2, λ^*, θ_f, $\xi_1/\sqrt{\tau}$ and $\xi_2/\sqrt{\tau}$. In this case with $T_{a1} = T_{a2}$, the knowledge of $\xi_1/\sqrt{\tau}$ is sufficient due to symmetry. Again, the discrepancies in the location of the points in the figure reflect numerical errors at the beginning of the calculations which diminish rapidly. A check for convergence was made by recomputing the interface travel and the temperature distribution

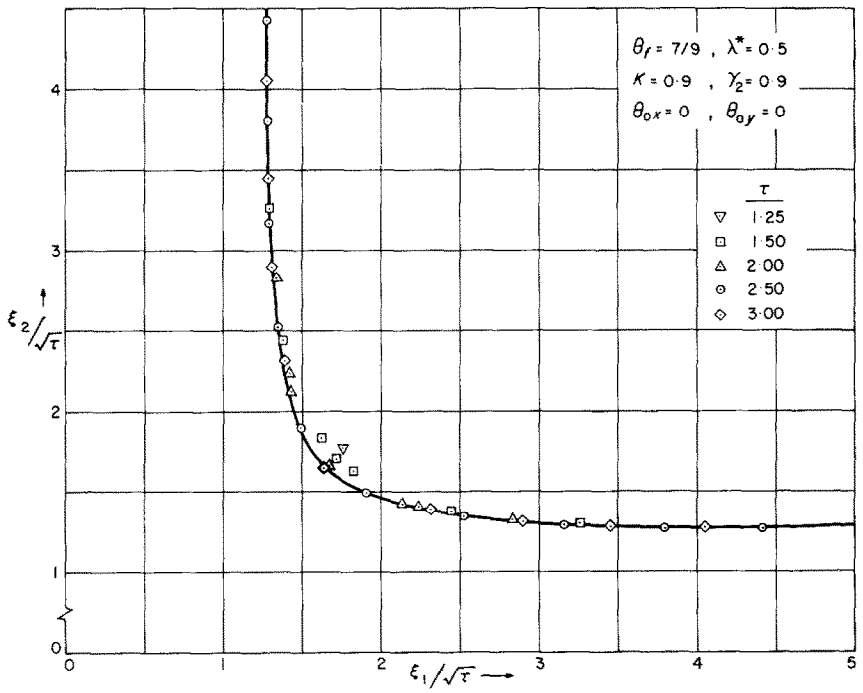

FIG. 8. Similarity solution for a long metal corner casting initially at a uniform temperature above the melting point and with prescribed boundary temperatures.

Symmetry conditions make it possible again to consider only one quarter of the section as in the previous example. Figure 8 shows the similarity solution for the data $\kappa = 0{\cdot}9$, $\gamma_2 = 0{\cdot}9$, $\lambda^* = 0{\cdot}5$, $\theta_f = 7/9$, and $\theta_{0x} = \theta_{0y} = 0$, where θ_{0x} and θ_{0y} are the dimensionless boundary temperatures prescribed along the lines $\xi_2 = 0$ and $\xi_1 = 0$, respectively. This result is comparable to the Neumann solution of the one-dimensional solidification problem in which the history in the medium with $\Delta\tau = 0{\cdot}008$ and $\Delta\tau = 0{\cdot}001$. The results were identical in all cases to the degree of accuracy required (third or fourth decimal place). Finally, in Fig. 9 a variation of this problem is presented, where the same data are used with the exception that the boundary temperatures are not equal, viz. $\theta_{0x} = 0$ and $\theta_{0y} = 2/9$.

Example 3. A liquid metal is poured into a cast of square cross-section. It is required to

study the freezing process in the cast if it is initially at a uniform temperature above the melting point ($\theta_f < 1$) and it is suddenly exposed to an ambient temperature, T_a, lower than the fusion temperature, through a prescribed heat-transfer coefficient, h. End effects are assumed negligible (infinite corner).

obvious and it is verified explicitly with reference to Figs. 13 and 14 where the interface positions along the diagonal and at infinity are plotted versus the Biot number.

Example 4. *A three-dimensional problem.* A liquid initially at the melting point is cast in a cubical enclosure. It is required to study the

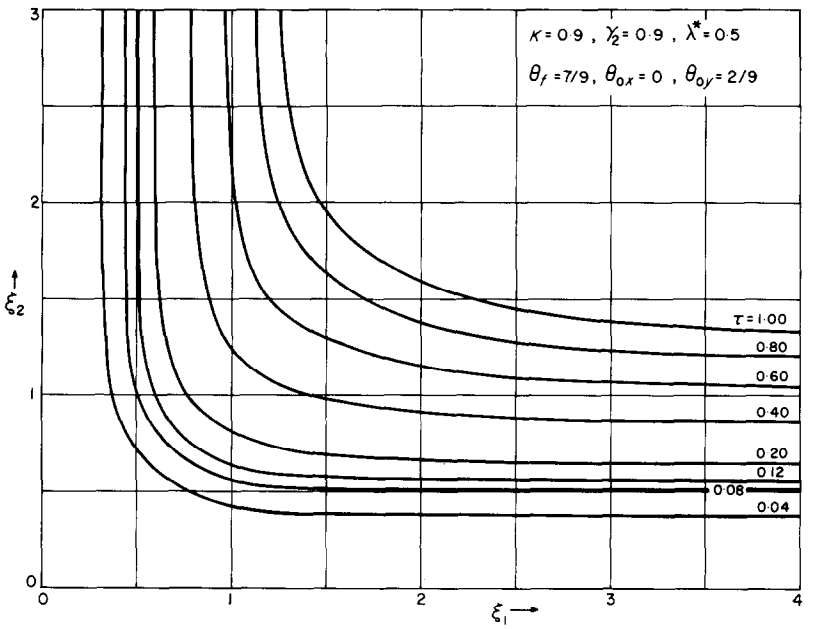

FIG. 9. Loci of interface at various values of the time for a long metal corner casting initially at a uniform temperature above the melting point and with two different values prescribed at the two boundaries.

The interface is graphed in Fig. 10 as a function of time for the data set of $\kappa = 0{\cdot}9$, $\gamma_2 = 0{\cdot}9$, $\lambda^* = 0{\cdot}5$ and $\theta_f = 7/9$. The Biot number is chosen to be equal to $Bi = 2$.

The convergence of the method is again examined. Thus, using the same data with different values of the prescribed Biot number at the boundaries, plots similar to those of Fig. 10 were drawn locating the interface. Figures 11 and 12 follow from those graphs; they, in turn, show the progress of solidification along the diagonal and on a line far from the corner, respectively, for various values of the Biot number. The convergence of the solution is

solidification process in the cast if its surface is maintained at a constant temperature (only the corner effect is to be studied).

The nature of the interface motion is shown in Figs. 15–18. The data used were $\lambda^* = 1{\cdot}5613$ and $\theta_f = 1$. The first four of these figures are graphs of the interface at different times on planes parallel to one of the boundary planes (in this case on the planes $\xi_3 = 1, 2$ and 3). The last figure is a plot of the same on the diagonal plane. These results are as expected; in fact, the plot for station $\xi_3 = 4$ is identical with Fig. 4 of the first example which is the two-dimensional counterpart of this problem. That figure repre-

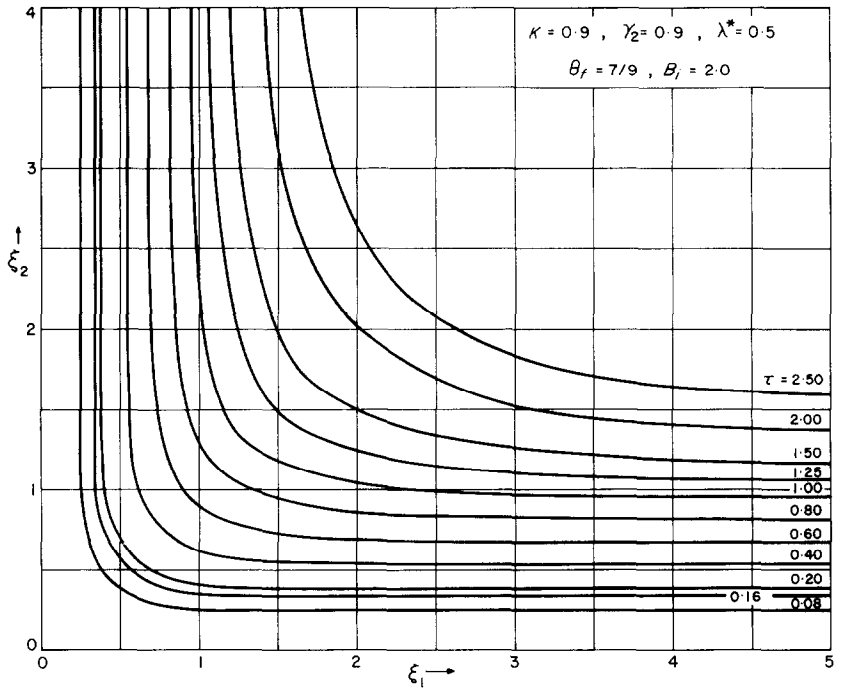

FIG. 10. Interface positions at several values of time for a long metal corner casting initially at a uniform temperature above the melting point and subjected to Newtonian cooling.

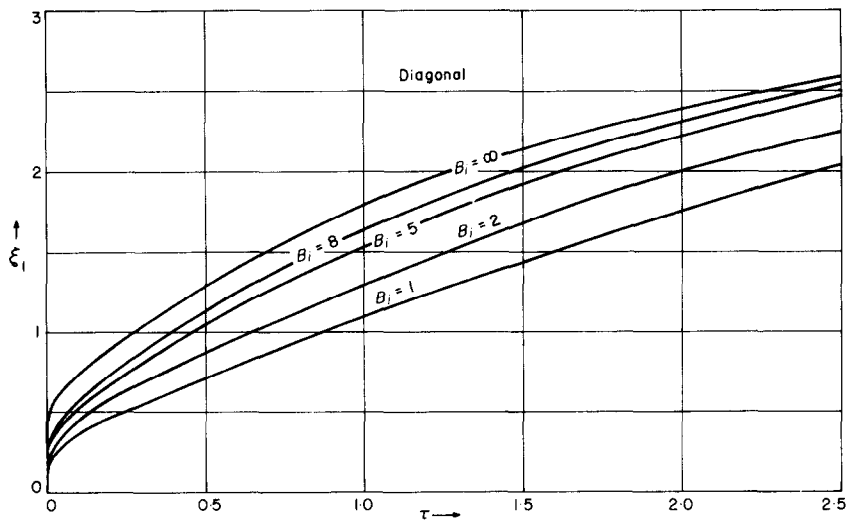

FIG. 11. Progress of solidification front along the diagonal of the corner of Fig. 10 for various values of the Biot number.

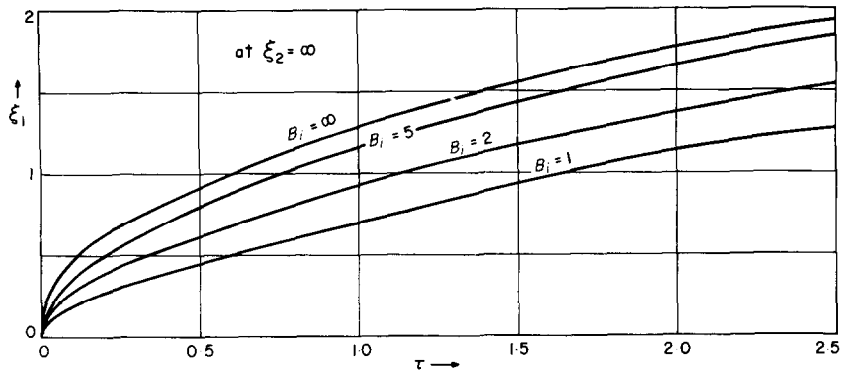

FIG. 12. Progress of solidification front along a line at infinite distance from the corner of the problem of Fig. 10 for various values of the Biot number (one-dimensional solution).

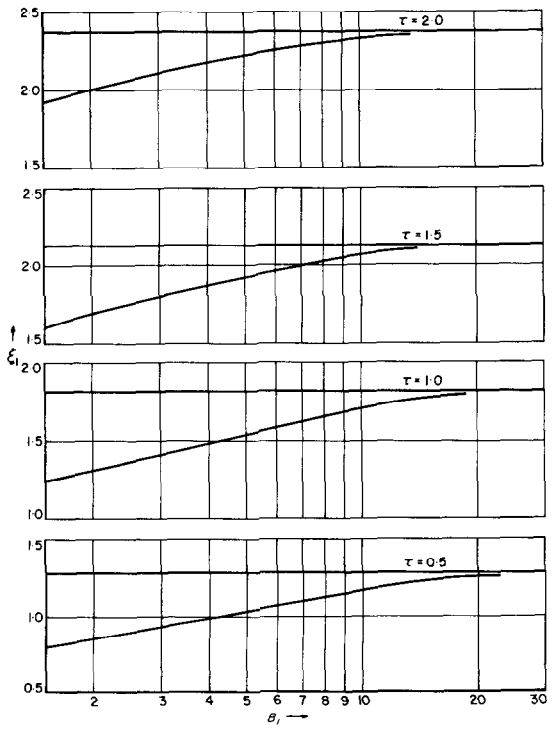

FIG. 13. Interface location along the diagonal at $\tau = 0.5$, 1·0, 1·5 and 2·0 vs. the Biot number for the problem of Fig. 10.

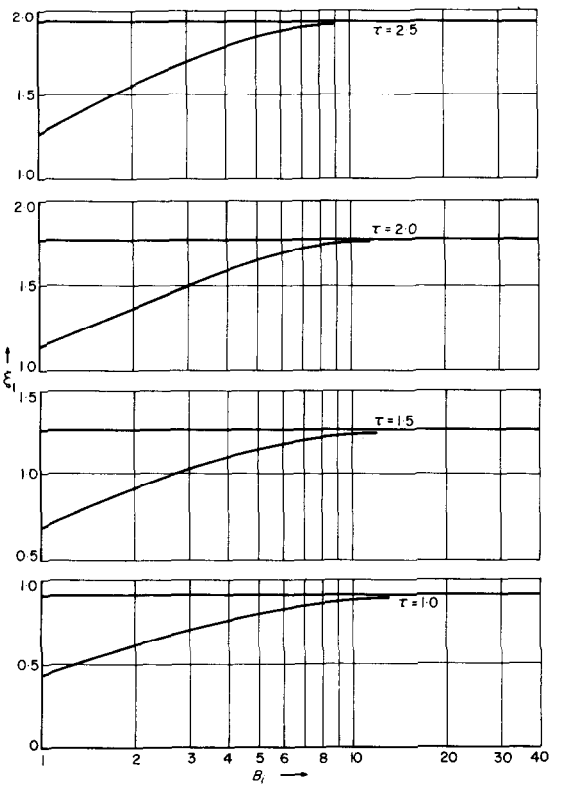

FIG. 14. Interface position along a line at infinite distance from the corner of the problem of Fig. 10 at $\tau = 1.0$, 1·5, 2·0 and 2·5 vs. the Biot number (one-dimensional solution).

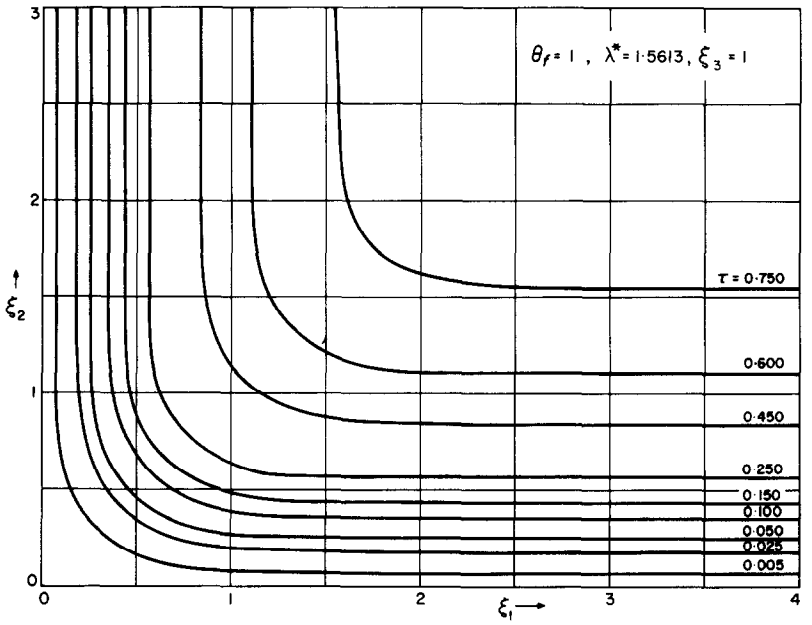

FIG. 15. Loci of interface in the plane $\xi_3 = 1$ at various values of the time for a three-dimensional long corner initially at the fusion temperature and having a prescribed temperature on all the fixed boundaries.

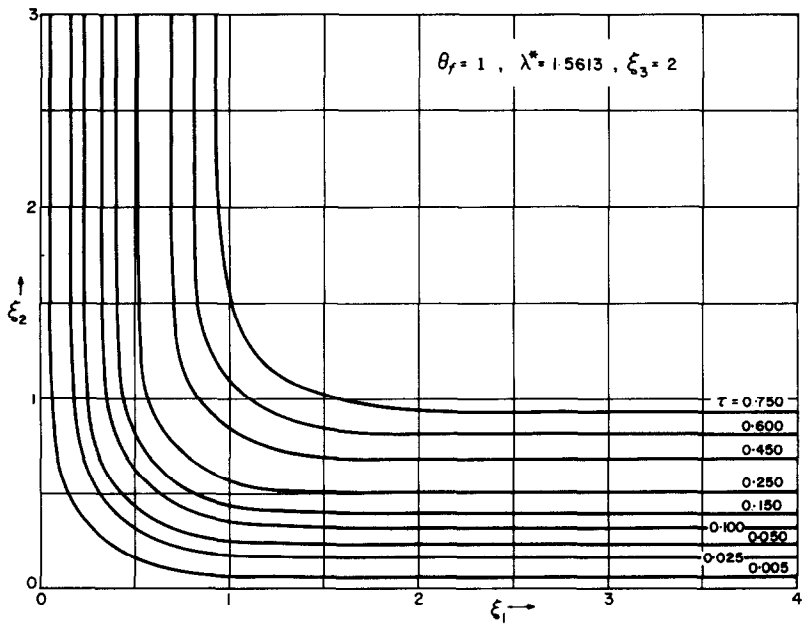

FIG. 16. Loci of interface in the plane $\xi_3 = 2$ at various values of the time for the three-dimensional problem described in Fig. 15.

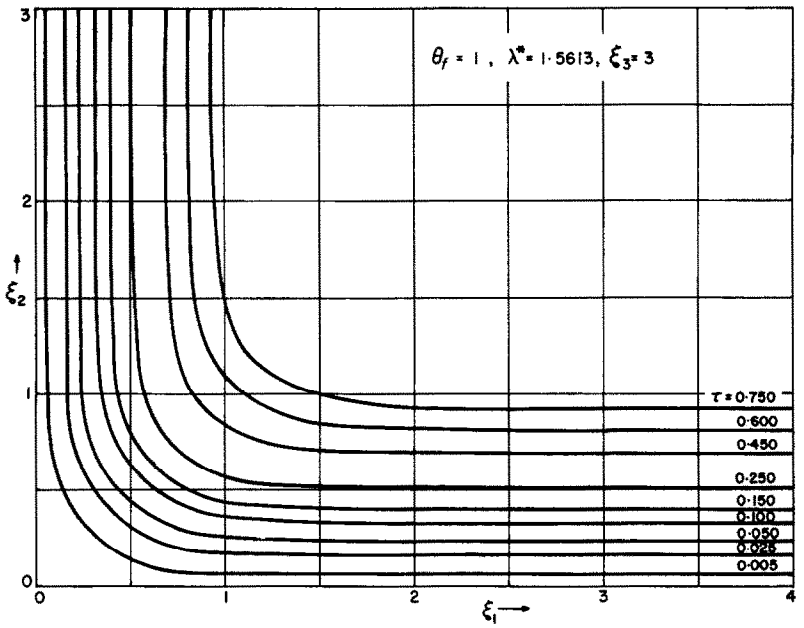

FIG. 17. Loci of interface in the plane $\xi_3 = 3$ at various values of time for the three-dimensional problem described in Fig. 15.

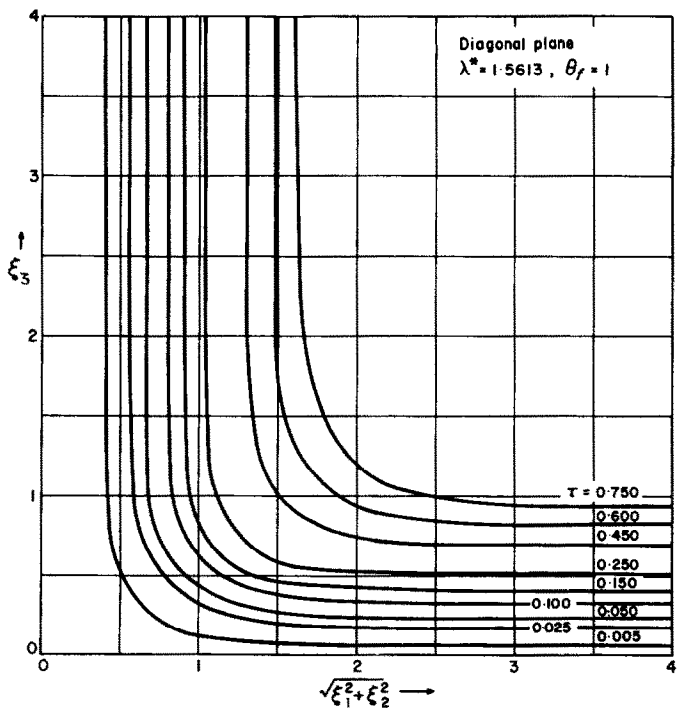

FIG. 18. Loci of interface in the diagonal plane at several values of the time parameter for the three dimensional problem of Figs. 15–17.

sents the interface travel on a plane located far enough from the corner so that it is not subject to its effects, yet.

CONCLUSIONS

The foregoing sample problems have been selected to cover cases involving configurations of both two and three dimensions and containing typical boundary conditions encountered frequently in practice. Unfortunately, examples 2–4 could not be compared with other published work since this is not available in the literature. It is reasonable to conclude, however, that the method presented in this manuscript is generally applicable to all geometries and boundary conditions and that the results obtained here are sufficiently accurate for engineering use. The computational procedure has been found to be reasonably facile, and this is verified by the speed of the computer calculations; the average computation time on the IBM 360-75 Model for a practical number of time steps (1000 or more) was in the vicinity of 1–2 min.

As a final comment, it is worth indicating that the assumption of pure conduction is not strictly correct, but experience has shown that, for a number of metallic castings, this model represents the physical conditions satisfactorily [19]. To determine the applicability of this assumption, an order of magnitude study was performed which indicated that the primary mode of heat transfer in the melt was conduction, although convection might be of importance in some cases. The relative importance of convection versus conduction in a solidifying melt, which seems to depend, among other factors, on the physical properties of the substance involved, remains the subject of further study.

ACKNOWLEDGEMENTS

The author wishes to express his gratitude to Dr. P. Razelos for his interest and advice and to Prof. H. G. Elrod, Jr. for his constant guidance and his invaluable criticisms during the course of this research. Special thanks are also due to the administration and the staff of the Columbia University Computer Center for the permission to use its facilities and the assistance provided in the course of the numerical computations. The financial assistance of the Heat and Mass Transfer Laboratory of Columbia University is appreciated.

REFERENCES

1. H. S. Carslaw and J. C. Jaeger, *Conduction of Heat in Solids*, Chapter 11. Clarendon Press, Oxford (1959).
2. H. G. Landau, Heat conduction in a melting solid, *Q. Jl Appl. Math.* **8**, 81–94 (1950).
3. J. C. Muehlbauer and J. E. Sunderland, Heat conduction with freezing or melting, *Appl. Mech. Rev.* **18**, 951–959 (1965).
4. H. G. Elrod, Freezing and remelting of radioactive material on cold, vertical pins, NDA Memo 14-181 (1957).
5. L. C. Tao, Generalized numerical solutions of freezing a saturated liquid in cylinders and spheres, *A.I.Ch.E. Jl* **13**, 165–169 (1967).
6. L. T. Rubenstein, Heat transfer in a two-phase medium in the case of cylindrical symmetry, *Dokl. Akad. Nauk U.S.S.R.* **79**, 945–948 (1951).
7. G. S. Springer and D. R. Olsen, Method of solution of axisymmetric solidification and melting problems, ASME Paper 62-WA-246 (1962).
8. J. M. Lederman, Axisymmetric melting or solidification of cylindrical bodies, Doctoral Dissertation, Columbia University (1968).
9. D. Langford, The freezing of spheres, *Int. J. Heat Mass Transfer* **9**, 827–828 (1966).
10. P. B. Grimado, Symmetric melting and solidification of spheres, Doctoral Dissertation, Columbia University (1968).
11. A. B. Datsev, On the two-dimensional Stefan problem, *Dokl. Akad. Nauk U.S.S.R.* **101**, 441–444 (1955).
12. D. N. de G. Allen and R. T. Severn, The application of relaxation methods to the solution of non-elliptic partial differential equations, *Q. Jl Mech. Appl. Math.* **15**, 53–62 (1962).
13. G. Poots, An approximate treatment of a heat conduction problem involving a two-dimensional solidification front, *Int. J. Heat Mass Transfer* **5**, 339–348 (1962).
14. D. L. Sikarskie and B. A. Boley, The solution of a class of two-dimensional melting and solidification problems, *Int. J. Solids Struct.* **1**, 207–234 (1965).
15. A. Lazaridis, A numerical solution of the solidification (or melting) problem in multidimensional space, Doctoral Dissertation, Columbia University (1969).
16. P. D. Patel, Interface conditions in heat conduction problems with change of phase, *AIAA Jl* **6**, 2454 (1968).
17. F. C. Lockwood, Simple numerical procedure for the digital computer solution of non-linear transient heat conduction with changes of phase, *J. Mech. Engng Sci.* **8**, 259–263 (1966).
18. G. M. Dusinberre, A note on the implicit method for finite difference heat transfer calculations, *Trans. Am. Soc. Mech. Engrs* **83C**, 92 (1961).
19. V. Paschkis, Personal Communication.

UNE SOLUTION NUMÉRIQUE DU PROBLÈME DE LA SOLIDIFICATION (OU DE LA FUSION) MULTIDIMENSIONNELLE

Résumé—Le but de cette étude était d'établir une technique numérique simple avec laquelle on puisse traiter les problèmes de transport de chaleur faisant intervenir un changement de phase. Les problèmes sont non linéaires à cause des conditions à l'interface en mouvement. Le schéma numérique présenté ici résout les équations appropriées au problème multidimensionnel et détermine la distribution de température dans les deux milieu autour de l'interface liquide solide en même temps qu'il donne le lieu de cette dernière au cours du temps.

Les types de conditions aux limites rencontrées le plus fréquemment en pratique sont étudiés dans l'analyse; les problèmes pris comme exemples sont choisis de telle façon qu'ils représentent les conditions de la température constante et du refroidissement selon la loi de Newton à la frontière de la substance en train de se solidifier. La plaque bidimensionnelle et les coins bi- et tridimensionnels sont employés pour donner des examples de géométries multidimensionnelles typiques.

La comparison des résultats obtenus ici avec les quelques solutions existantes montrent un accord satisfaisant.

EINE NUMERISCHE LÖSUNG DES MEHRDIMENSIONALEN ERSTARRUNGS- (ODER SCHMELZ-) VORGANGS

Zusammenfassung—Es war der Zweck dieser Untersuchung ein einfaches numerisches Rechenverfahren zu entwickeln mit dem Wärmeübertragungsprobleme einschliesslich der Phasenübergänge behandelt werden können. Diese Probleme sind wegen der wandernden Phasengrenzfläche nicht linear. Das numerische Schema liefert die Lösungen der beschreibenden Gleichungen für das mehrdimensionale Problem und berechnet die Temperaturverteilungen in den Medien zu beiden Seiten der Phasengrenzfläche, gleichzeitig wird der Ort der Phasengrenzfläche mit fortschreitender Zeit ermittelt.

Die in der Praxis am häufigsten vorkommenden Randbedingungen wurden untersucht, die Beispiele sind so ausgewählt, dass sie konstante Temperatur und Newtonische Abkühlungs-Bedingungen an der Grenze der erstarrenden Substanz widerspiegeln. Die zweidimensionale Platte und die zwei- oder dreidimensionale Ecke sind als Beispiele für typische mehrdimensionale Geometrien verwendet.

Vergleiche der erhaltenen Ergebnisse mit den wenigen existierenden Lösungen zeigen eine zufriedenstellende Übereinstimmung.

ЧИСЛЕННОЕ РЕШЕНИЕ МНОГОМЕРНЫХ ЗАДАЧ ОТВЕРДЕНИЯ (ПЛАВЛЕНИЯ)

Аннотация—Целью этого исследования было создать простой численный метод решения задач теплообмена с фазовым изменением. Эти задачи нелинейные из-за условий у поверхности движущейся границы раздела фаз. По приведенной здесь численной схеме решаются соответствующие уравнения для многомерной задачи и определяется распределение температуры в жидкой и твёрдой фазах, а также изменение положения границы раздела со временем.

Анализируются наиболее часто встречающиеся на практике граничные условия. Задачи подобраны таким образом, чтобы учесть постоянную температуру и условия ньютоновского охлаждения на границе отвердевающего вещества. Двумерная плита и двух- и трёхмерные углы используются в качестве примера характерной многомерной геометрии.

Сравнение результатов, полученных в данной работе, с несколькими имеющимися решениями, показывает удовлетворительное соответствие.